Research Paper

Screening of Lipid Carriers and Characterization of Drug-Polymer-Lipid Interactions for the Rational Design of Polymer-Lipid Hybrid Nanoparticles (PLN)

Yongqiang Li,[1] Nicolas Taulier,[1] Andrew M. Rauth,[2] and Xiao Yu Wu[1,3]

Purpose. The thermodynamics and solid state properties of components and their interactions in a formulation for polymer-lipid hybrid nanoparticles (PLN) were characterized for screening lead lipid carriers and rational design of PLN.

Methods. Verapamil HCl (VRP) was chosen as a model drug and dextran sulfate sodium (DS) as a counter-ionic polymer. Solubility parameters of VRP, VRP-DS complex, and various lipids were calculated and partition of VRP and VRP-DS in lipids was determined. Thermodynamics of VRP binding to DS was determined by isothermal titration calorimetry (ITC). The solid state properties of individual components and their interactions were characterized using differential scanning calorimetry (DSC) and powder X-ray diffraction (PXRD).

Results. Dodecanoic acid (DA) was identified as the best lipid carrier among all lipids tested based on the solubility parameters and partition coefficients. VRP-DS complexation was a thermodynamically favorable process. Maximum binding capacity of DS and the highest drug loading capacity of DA were obtained at an equal ionic molar ratio of DS to VRP. In the PLN formulation, DA remained its crystal structure but had a slightly lower melting point, while VRP-DS complex was in an amorphous form.

Conclusions. Drug loading efficiency and capacity of a lipid matrix depend on the VRP-DS binding and the interactions of the complex with the lipid. A combined analysis of solubility parameters and partition coefficients is useful for screening lipid candidates for PLN preparation.

KEY WORDS: drug-polymer complex; isothermal titration calorimetry; partition coefficient; polymer-lipid hybrid nanoparticles (PLN); solid lipid nanoparticles; solubility parameters.

INTRODUCTION

Solid lipid nanoparticles (SLN) have attracted increasing attention in the past decade as an alternative dosage form to microemulsions, liposomes, and polymeric nanoparticles (1–11). The submicron sized particles and solid state of physiological lipid carriers favor the pharmaceutical and biopharmaceutical applications of SLN. However, common drawbacks of SLN such as low drug loading capacity, high initial burst release kinetics and drug leakage during storage still demand to be addressed (5). It is well known that the

properties of SLN are correlated with the physicochemical and solid state properties of its components such as drug and lipid, and the partition behavior of the drug between lipid and aqueous phases (6,7). Nevertheless, to date, detailed rules for selection of lipid candidates have not been well defined and the popular approach remains a trial-and-error process, because of the complexity of the system.

Previous applications of SLN mainly focus on the delivery of poorly water-soluble drugs due to the highly hydrophobic nature of the lipid carriers. In order to deliver hydrophilic drugs, organic salts have been used as counter ions to incorporate highly water-soluble drugs into SLN (8–10). Our group has exploited the characteristic chemical structure of anionic polymers (polyelectrolyte) to develop a polymer-lipid hybrid nanoparticle (PLN) system, a variation of SLN (11), and demonstrated enhanced cytotoxicity against multidrug resistant cancer cells by the PLN loaded with antineoplastic and chemosensitizing agents (12,13). Previous studies have revealed that both drug–polymer complexation and the nature of the lipid played critical roles in drug incorporation and release profile of PLN. However, the thermodynamics of drug-polymer binding, the interactions of involved components and their effect on the solid state properties of PLN have not been studied. Thus the mecha-

[1] Leslie Dan Faculty of Pharmacy, University of Toronto, Toronto, ON M5S 2S2, Canada.

[2] Experimental Therapeutics, Ontario Cancer Institute, Toronto, ON M5G 2M9, Canada.

[3] To whom correspondence should be addressed. (e-mail: xywu@phm.utoronto.ca)

ABBREVIATIONS: DA, dodecanoic acid; DDI, distilled and deionized; DS, dextran sulfate sodium salt; DSC, differential scanning calorimetry; ITC, isothermal titration calorimetry; MP, melting point; PLN, polymer-lipid hybrid nanoparticles; PXRD, powder X-ray diffraction; SLN, solid lipid nanoaprticles; VRP, verapamil HCl; VRP-DS complex, the complex of verapamil HCl and dextran sulfate sodium salt.

nisms of drug loading and release are still poorly understood, which hampers rational design of PLN.

The interactions and miscibility between drugs and excipients have been investigated by thermal and non-thermal methods such as differential scanning calorimetry (DSC) and powder X-ray diffraction (PXRD) to predict the optimal compositions of different dosage forms including SLN (14–20). Similar approaches can be employed to examine the solubility or miscibility of drug-polymer complex in a molten lipid. Yet the experimental approach to screening lipid candidates is costly, labor intensive and time-consuming. On the other hand, the use of theoretical solubility parameters (or cohesive energy densities) (21,22) may provide an early, quick screening tool for selection of lipid candidates. Based on the rule of 'like dissolves in like', the best miscibility of a drug and an excipient is expected when both materials possess similar total solubility parameters and polarities (including additive effect of hydrogen-bonding) (23).

In the present study, solubility parameters were applied for the first time to screen lipid carrier for the design of PLN, on the basis of group contributions (24,25). Complementary to the theoretical calculations, partition experiments were employed to verify the solubility or miscibility of drug-polymer complex in various lipids and to optimize the ionic molar ratio of polymer to drug. In addition, solid state properties of involved components and their interactions in different forms were characterized by using differential scanning calorimetry (DSC) and powder X-ray diffraction (PXRD). The thermodynamics of drug-polymer complexation was determined by isothermal titration calorimetry (ITC) (26).

Verapamil HCl (VRP), with a structure shown in Scheme 1a, was chosen as a model drug. It is a calcium channel blocker and chemosensitizer of P-glycoprotein-mediated drug resistance. VRP dissolves in water with a solubility of 50 mg/ml described by the supplier. Low-molecular-weight dextran sulfate sodium salt (DS), a modified natural polysaccharide depicted in Scheme 1b, was used as a counterion polymer. For rational design of PLN, this work was focused on three objectives: (1) to screen a lead lipid candidate for PLN preparation using theoretical solubility parameters and partition experiments; (2) to investigate the thermodynamics of DS and VRP complexation; and (3) to characterize the solid state properties of each component of PLN and their interactions by calorimetry and crystallography.

MATERIALS AND METHODS

Materials

Verapamil HCl, stearic acid (MP: 67–72°C), palmitic acid (MP: 61–62.5°C), myristic acid (MP: 52–54°C), dodecanoic acid (MP: 44–46°C), tribehenin (MP: 80–85°C) and dextran sulfate sodium salt (MW: 5,000) were purchased from Sigma-Aldrich Canada (Oakville, Ontario, Canada). Tristearin (MP: 72–75°C) was obtained from Fluka AG (Buchs, Switzerland). Compritol ATO 888 (a mixture of approximately 15% mono-, 50% di- and 35% triglycerides of behenic acid, MP: 69–74°C) and Precirol ATO 5 (MP: 50–60°C) were kind gifts from Gattefossé Inc. (Toronto, Ontario, Canada). Precirol ATO 5 is

a   Verapamil HCl
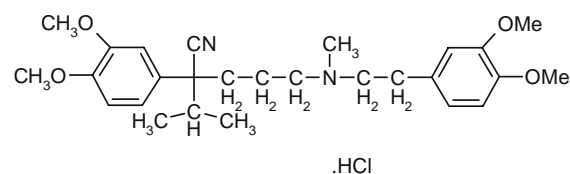
b   Dextran sulfate sodium salt
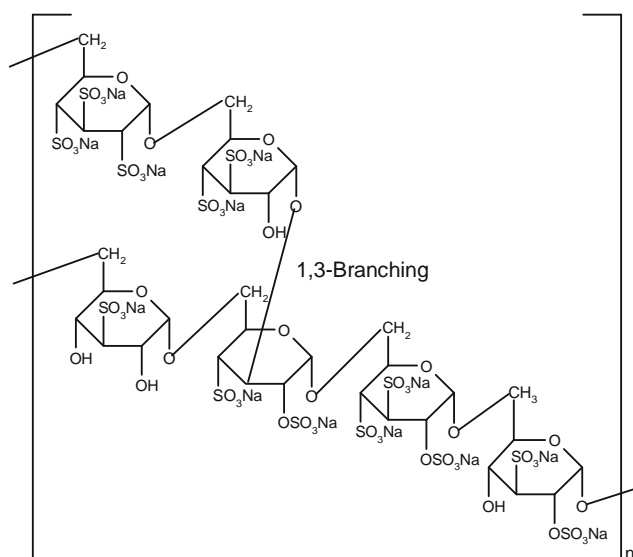
Scheme 1. Chemical structures of verapamil HCl and dextran sulfate sodium salt. (a) Verapamil HCl (b) Dextran sulfate sodium salt.

a mixture of approximately 8–22% mono-, 40–60% di-, and 25–35% triglycerides of palmitic acid and stearic acid, fatty acids other than palmitic acid and stearic acid account for less than 10%. $CaCl_2$ and 1-octanol was purchased from Fisher Chemicals (Pittsburgh, PA, U.S.A.). Distilled and deionized (DDI) water was prepared with a Milli-Q water system (Milli-Pore, Canada).

Methods

Calculation of Total Solubility Parameters

The total solubility parameter (δ_{total}) is a measure of cohesive energy of a substance introduced by Hansen (27). It comprises three components that represent specific inter-atomic or intermolecular forces between a solvent and a solute:

$$\delta_{\text{total}}^2 = \delta_{\text{d}}^2 + \delta_{\text{p}}^2 + \delta_{\text{h}}^2 \tag{1}$$

where δ_{d}, δ_{p} and δ_{h} are the partial solubility parameters associated with the dispersion forces, the polar interactions and the hydrogen bonding, respectively.

The values of δ_{d}, δ_{p} and δ_{h} cannot be determined directly. Nevertheless, based on the knowledge of the

chemical structure of specific substances, partial solubility parameters can be predicted by using the method of group contributions proposed by Van Krevelen (25):

$$\delta_{d} = \frac{\sum F_{d}}{\sum V} \qquad (2)$$

$$\delta_{p} = \frac{\sqrt{\sum F_{p}^{2}}}{\sum V} \qquad (3)$$

$$\delta_{h} = \frac{\sqrt{\sum E_{h}}}{\sqrt{\sum V}} \qquad (4)$$

where F_{d}, F_{p}, E_{h} are, respectively, the group contribution to dispersion forces, polar forces, hydrogen bond energy, and V is the molar volume.

Correspondingly, the mixing enthalpy (ΔH_{M}) *per* unit volume between compound 1 and compound 2 becomes:

$$\Delta H_{M} = \Phi_{1} \Phi_{2} \left[(\delta_{d1} - \delta_{d2})^{2} + (\delta_{p1} - \delta_{p2})^{2} + (\delta_{h1} - \delta_{h2})^{2} \right] \qquad (5)$$

where Φ_{1} and Φ_{2} are the volume fractions of component 1 and component 2, respectively.

The polarity of a substance (X_{p}) can be defined as follows to account the contribution from hydrogen bonding and other polar interactions (28):

$$X_{p} = 1 - \frac{\delta_{d}^{2}}{\delta_{total}^{2}} \qquad (6)$$

In the present study, partial and total solubility parameters and polarity of a total of 15 lipids, one solvent, and the VRP-DS complex were calculated using Eqs. (2), (3), (4) and (6), with the values of F_{d}, F_{p}, E_{h}, and V of specific function groups being obtained from literature (25). The enthalpy of mixing between the lipids and the complex was calculated based on Eq. (5).

Preparation of VRP-DS Complex

The VRP-DS complex was prepared by the co-precipitation method (29). Under constant stirring, aliquots of a DS solution were added to a VRP solution at 25°C slowly to obtain the specific ionic molar ratio of DS to VRP. The precipitate was collected through centrifugation, washed several times using DDI water and then lyophilized for 24 h. The freeze dried sample was ground for future analysis.

Determination of Partition of VRP-DS Complex in Different Lipids

Apparent partition coefficients of VRP-DS complex between lipid and aqueous phase were measured to study the solubility of the complex in the lipid phase and to select lead candidates for PLN formulation. Compritol ATO 888, Precirol ATO 5, tribehenin, tristearin, stearic acid, palmitic acid, myristic acid, dodecanoic acid, and 1-octanol were tested as the lipid phase. In a typical partition experiment,

10 mg of VRP were dispersed in a mixture of 1 g of a molten lipid and 1 ml of DDI water, which was kept at a temperature 5°C above the melting point of the lipid by a water bath. Known amounts of DS were added slowly to the mixture to achieve desirable ionic molar ratios of DS to VRP. The mixture was stirred for 45 min at the same temperature, and then left still for another 45 min to allow the partition to reach equilibrium. After cooling, the tube was shaken vigorously and the aqueous phase was collected. 1 ml of a diluted aqueous sample was incubated with the same volume of 0.3 M $CaCl_{2}$ solution for 24 h at room temperature. The VRP content in the aqueous solution was then analyzed with a UV–vis spectrophotometer (Hewlett-Packard 8452A, Palo Alto, CA) at a wavelength of 278 nm. The control experiment was conducted as follows: aliquots of DDI water were used to wash the tube, collected and then incubated with 0.3 M $CaCl_{2}$ solution for VRP analysis. The apparent partition coefficients were calculated as the ratio of the amount of VRP in lipid to the residual amount of VRP in the aqueous phase at equilibrium.

For thermal and crystallographic characterization, the lipid phase with incorporated VRP-DS complex at the optimal ionic molar ratio of DS to VRP was separated from the aqueous phase, lyophilized and ground using a mortar and a pestle.

Isothermal Titration Calorimetry

The heat of VRP and DS complexation was determined by isothermal titration calorimetry (ITC) at 25°C using a CSC 4200 isothermal titration calorimeter (Calorimetric Sciences Corp., Lindon, UT, U.S.A.). The instrument was calibrated with a 500 μJ electrical pulse and by measuring the enthalpy of $BaCl_{2}$ with 18-crown-6. In order to maintain a procedure similar to that used in the PLN preparation, a solution of 2.7 mg/ml DS was injected in an increment of 10 μl every 400 s into a stirred sample cell filled with 1 ml of 1 mg/ml VRP. To measure the heat involved in the dilution of DS solution and dilution of VRP solution, 1 ml of DDI water and 1 ml of 1 mg/ml VRP solution were titrated with 2.7 mg/ml DS solution and DDI water, respectively. The heat released by the addition of the solvent (i.e., DDI water) was evaluated by titrating DDI water with DDI water. The heat released for each titration was calculated by integration of the peak area.

The binding constant, enthalpy and stiochiometry of interaction for DS association with VRP were determined with an independent binding site model (30). In this model, the total heat of binding, Q (μJ), is expressed as:

$$Q = n\alpha[Drug]V\Delta H_{b} \qquad (7)$$

where n is the reciprocal of number of independent binding sites on one molar monomer unit of the polymer, [Drug] is the drug concentration (mol/L), V is the drug volume in the sample cell (L), ΔH_{b} is the binding enthalpy (μJ/mol), and α is the fractional saturation of the binding sites that can be derived from the following quadratic equation:

$$\alpha^{2} - \alpha \left(1 + \frac{[Polymer]}{n[Drug]} + \frac{1}{nK_{b}[Drug]} \right) + \frac{[Polymer]}{n[Drug]} = 0 \qquad (8)$$

where [Polymer] is the accumulated concentration (mol/l) of polymer after each titration, K_b is the binding constant (M^{-1}).

The values of ΔH, K_b and n were estimated by fitting Eqs. (7) and (8) to the ITC data using the software ORIGIN (Microcal, Northhampton, MA, U.S.A.).

To exclude the possible additive heat involved in the precipitation of the complex, 120 μl of 2.7 mg/ml DS was injected into 1 ml of 1 mg/ml VRP solution slowly under constant stirring. The intensity of the solution, as a measure of particle formation, was then determined by using a Nicomp 380 submicron particle sizer (Particle Sizing Systems Inc., Santa Barbara, CA, U.S.A.). The reason for using this instrument instead of a spectrophotometer is that the intensity signal is very sensitive to the presence or formation of dilute colloidal particles.

Differential Scanning Calorimetry (DSC)

Thermal analysis was conducted using DSC 2010 differential scanning calorimeter (TA Instruments, New Castle, DE, U.S.A.). The temperature and heat flow calibrations were performed at a heating rate of 5°C/min from −20 to 250°C with indium (purity >99.999%) as a standard substance. Then powder samples of 10–15 mg each were analyzed at the same settings under a purge of nitrogen (50 ml /min). Each analysis was performed in triplicate.

Powder X-ray Diffraction (PXRD)

Powder X-ray diffraction of various samples of 200 mg each was measured at room temperature with a Siemens D5000 θ/2θ diffractometer (Karlsruhe, Germany). The common Cu–Kα radiation source was operated at a voltage of 50 kV and a current of 35 mA, and the secondary beam was monochromatized by a Kevex solid state detector. The samples were scanned from 2° to 55° (2θ) with a step size of 0.02° and a step interval of 1.2 s. The data were processed by DiffracPlus™ software.

Statistical Analysis

Statistical comparison of two independent means (or two independent groups) was performed by using a two-sided Student *t*-test. A value of $p < 0.05$ was considered to be statistically significant. All values were expressed as the mean value±standard deviation (S.D.) of three independent experiments. Statistical analyses were implemented by using SAS software (version 8.0).

RESULTS

Solubility Parameters of the Lipids and the VRP-DS Complex

Listed in Table I are the calculated three partial solubility parameters, the total solubility parameters and polarity of 15 lipids, 1-octanol and the VRP-DS complex, together with their chemical formulas. The lipids include fatty acids with different chain lengths, triglycerides with different structures, glycerol esters and mixtures of glycerol esters. Alkyl groups such as –CH₃, –CH₂–, >(CH)–, >C< contribute to the dispersion forces; while the groups –OH, –COOH, –O– and –COO– increase polar forces including hydrogen bonding. The polarity of fatty acids decreases from 0.15 to 0.090 when their aliphatic chain length increases from C_{12} to C_{20}. In comparison with their corresponding fatty acids, triglycerides possess less polarity due to the domination of alkyl groups. Hence, triglycerides are more suitable for loading poorly water-soluble drugs than fatty acids. Nevertheless, glyceryls in the mono- form, such as glyceryl behenate (mono-), possess stronger polarity than their corresponding fatty acids due to stronger hydrogen bonding between molecules. The contribution of hydrogen bonding to the polarities of glyceryl hydroxystearate and 1-octanol is also evident, with polarity of 0.39 and 0.35, respectively. The VRP-DS complex is quite hydrophilic with a polarity of 0.22, which can be attributed to the existence of many polar groups (e.g., –OH, –O–, –SO₂–, –CN).

Table I. Calculated Values of Partial Solubility Parameters, Total Solubility Parameter and Polarity of Various Lipids and the VRP-DS Complex

Compounds	Chemical formula	δ_d	δ_p	δ_h	δ_{total}	Polarity
Dodecanoic acid	$CH_3(CH_2)_{10}COOH$	16.37	1.88	6.7	17.78	0.15
Myristic acid	$CH_3(CH_2)_{12}COOH$	16.42	1.64	6.26	17.65	0.13
Palmitic acid	$CH_3(CH_2)_{14}COOH$	16.46	1.46	5.90	17.54	0.12
Stearic acid	$CH_3(CH_2)_{16}COOH$	16.49	1.31	5.59	17.46	0.11
Behenic acid	$CH_3(CH_2)_{18}COOH$	16.54	1.09	5.10	17.34	0.090
Caprylate triglycerides	$[CH_3(CH_2)_6COOCH_2]_2CHOCO(CH_2)_6CH_3$	16.64	1.78	6.64	18.00	0.15
Caprate triglycerides	$[CH_3(CH_2)_8COOCH_2]_2CHOCO(CH_2)_8CH_3$	16.66	1.48	6.06	17.79	0.12
Trilaurin	$[CH_3(CH_2)_{10}COOCH_2]_2CHOCO(CH_2)_{10}CH_3$	16.67	1.27	5.60	17.64	0.11
Trimyristin	$[CH_3(CH_2)_{12}COOCH_2]_2CHOCO(CH_2)_{12}CH_3$	16.69	1.11	5.24	17.52	0.090
Tripalmitin	$[CH_3(CH_2)_{14}COOCH_2]_2CHOCO(CH_2)_{14}CH_3$	16.70	0.98	4.94	17.44	0.083
Tristearin	$[CH_3(CH_2)_{16}COOCH_2]_2CHOCO(CH_2)_{16}CH_3$	16.70	0.88	4.68	17.37	0.075
Tribehenin	$[CH_3(CH_2)_{20}COOCH_2]_2CHOCO(CH_2)_{20}CH_3$	16.71	0.74	4.27	17.27	0.060
Glyceryl behenate (mono-)	$CH_3(CH_2)_{20}COOCH_2CHOHCH_2OH$	17.07	2.02	10.52	20.15	0.28
Glyceryl behenate (di-)	$[CH_3(CH_2)_{20}COOCH_2]_2CHOH$	16.81	1.08	6.57	18.08	0.14
Glyceryl hydroxystearate	$CH_3(CH_2)_5CHOH(CH_2)_{10}COOCH_2CHOHCH_2OH$	17.52	2.82	13.77	22.47	0.39
1-octanol	$CH_3(CH_2)_6CH_2OH$	16.13	3.20	11.32	19.96	0.35
VRP-DS complex*		19.97	3.04	10.03	22.55	0.22

* See Scheme 1 for the chemical structure of VRP and DS.

Table II. The Differences of Partial Solubility Parameters, Total Solubility Parameter, Mixing Enthalpy and Polarity Between Various Lipids and VRP-DS Complex

Compounds	$\Delta\delta_d$	$\Delta\delta_p$	$\Delta\delta_h$	$\Delta\delta_{total}$	ΔH_M	ΔPolarity
Dodecanoic acid	3.60	1.16	3.33	4.77	3.54	0.070
Myristic acid	3.55	1.40	3.77	4.90	4.37	0.090
Palmitic acid	3.51	1.58	4.13	5.01	5.21	0.10
Stearic acid	3.48	1.73	4.44	5.09	6.05	0.11
Behenic acid	3.43	1.95	4.93	5.21	7.62	0.13
Caprylate triglycerides	3.33	1.26	3.39	4.55	5.08	0.070
Caprate triglycerides	3.31	1.56	3.97	4.76	6.54	0.10
Trilaurin	3.30	1.77	4.43	4.91	7.90	0.11
Trimyristin	3.28	1.93	4.79	5.03	9.04	0.13
Tripalmitin	3.27	2.06	5.09	5.11	10.05	0.14
Tristearin	3.27	2.16	5.35	5.19	10.94	0.15
Tribehenin	3.26	2.30	5.76	5.28	12.27	0.16
Glyceryl behenate (mono-)	2.90	1.02	−0.49	2.40	1.94	−0.06
Glyceryl behenate (di-)	3.16	1.96	3.46	4.47	6.26	0.08
Glyceryl hydroxystearate	2.45	0.22	−3.74	0.090	3.67	−0.17
1-octanol	3.84	−0.16	−1.29	2.59	1.78	−0.13

Table II lists the differences in the partial solubility parameters, total solubility parameters and polarity between the VRP-DS complex and the lipids. The value of the mixing enthalpy (ΔH_M) between the complex and lipids indicates the amounts of energy required to achieve mutual solubility. Taking into account the differences in total solubility parameter and the polarity as well as the mixing enthalpy between the complex and the lipids, glyceryl behenate (mono-) and dodecanoic acid (DA) were identified as the most promising lipid candidates for loading of the VRP-DS complex. Although glyceryl behenate (mono-) has smaller differences with the VRP-DS complex, it only constitutes a small portion (15%) of Compritol ATO 888. Thus Compritol ATO 888 seems to be a poor choice for preparation of PLN. Nevertheless, the use of pure glyceryl behenate (mono-) as lipid candidate for PLN is worth of further exploration.

Partition of VRP-DS Complex in Various Lipids

As illustrated in Fig. 1, the highest partition coefficient is obtained with DA followed by myristic acid as the lipid phase at a drug loading level of 1% (w/w) and DS/VRP ionic molar ratio of 1.5. A significant difference exists between DA and myristic acid with $p < 0.001$. The order of partition coefficients for these lipids is: dodecanonic acid > myristic acid > palmitic acid > stearic acid > Precirol ATO 5 > Compritol ATO 888 > tristearin > tribehenin. The results of partition experiment are consistent with the calculated solubility parameters suggesting that DA has the best miscibility with the VRP-DS complex.

Using DA as the lipid matrix, the effect of the ionic molar ratio of VRP to DS on the partition behavior of the VRP-DS complex was studied. Figure 2 shows that a peak value of partition coefficient is obtained at the DS/VRP ionic molar ratio of 1.0. In other words, the partition of VRP-DS complex in the lipid phase is lower at DS/VRP ionic molar ratios smaller or greater than unity.

Table III summarizes drug loading efficiency and loading capacity, determined from the partition tests, as a function of drug to lipid ratio (w/w) with the DS/VRP ionic molar ratio being fixed at 1.0. The drug loading efficiency (DLE%) was calculated as the amount of VRP incorporated into the lipid divided by the amount of initial added drug, while drug loading capacity as the amount of drug loaded into lipid divided by the weight of the lipid, using the following equations:

$$\text{DLE\%} = \text{(Amount of VRP in lipid)} / \text{(Initial amount of VRP added)} \times 100\% \qquad (9)$$

$$\text{DLC\%} = \text{(Weight of VRP in lipid)} / \text{(Weight of lipid)} \times 100\% \qquad (10)$$

It is seen that as the drug to lipid ratio (w/w) is raised from 1:25 to 1:1, drug loading capacity of DA is improved from 3.95 to 88.07% (w/w), while the drug loading efficiency is still satisfactory with a value of 88.48%.
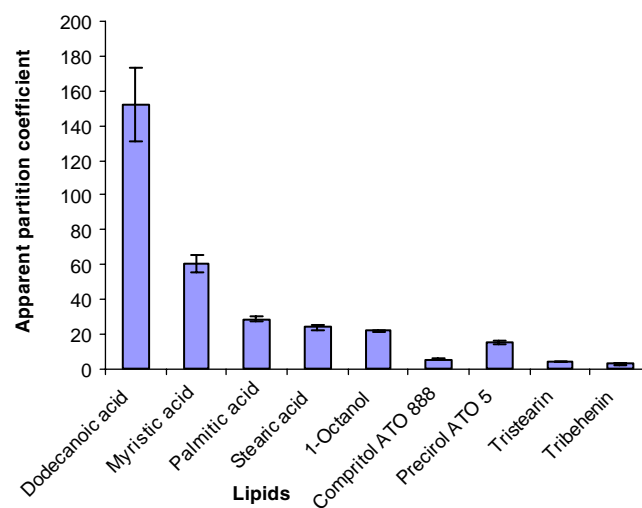

Fig. 1. Apparent partition coefficients of the drug-polymer complex in various lipids at a fixed ionic molar ratio of polymer to drug of 1.5. A significant difference exists between the result of dodecanoic acid as lipid phase and that of myristic acid as lipid phase ($p < 0.001$). *Error bars* are standard deviation for $n = 3$.
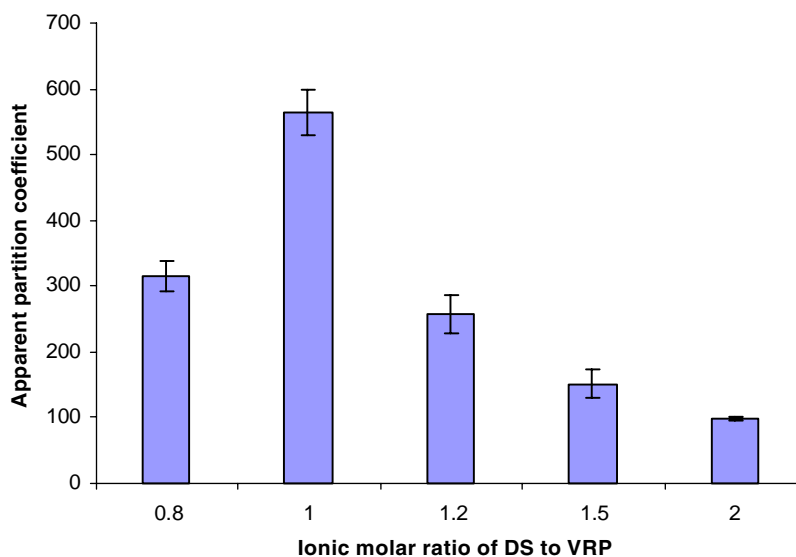
Fig. 2. Apparent partition coefficients of VRP-DS complex in dodecanoic acid *versus* ionic molar ratios of DS/VRP (*n* = 3). Significant differences exist between ionic molar ratio of DS to VRP at 0.8 and 1.0 (*p* < 0.001) as well as between 1.0 and 1.2 (*p* < 0.001). *Error bars* are standard deviation.

Energetics of VRP-DS Complexation

Figure 3a displays the rate of heat released due to the titration of VRP solution with DS. The large exothermic peaks in the first ten injections suggesting that all of the sulfate groups introduced in the early stage of the titration are bound to the drug. As the concentration of DS further increases, less amounts of VRP available for binding leads to less heat generated. The small peaks after full saturation is likely caused by dilution of DS and/or other non-specific effects. That calibrated heat released by complexation alone was calculated and plotted against the ionic molar ratio of DS to VRP (Fig. 3b). Since no particles were detected by the particle sizer, the possibility of an additive heat effect caused by the precipitation of the complex was excluded. Figure 3b illustrates that the maximum apparent heat change between two consecutive injections ($\Delta Q_{app} = Q_i - Q_{i-1}$) occurs immediately after the DS/VRP ionic molar ratio exceeds 1.0. This

means that below this ratio, all of the DS added are bound with VRP, while little titrant bound to VRP above it.

Figure 4 shows the fit of the cumulative heat *versus* DS/VRP ionic molar ratio by Eqs. (7) and (8). A good agreement between the predicted and the observed thermodynamic properties of VRP-DS complexation is evidenced with a Chi-square value of 0.05966. From data fitting, the values of K_b, ΔH_b and *n* were estimated to be 3.6×10^6 M^{-1}, -4.9 ± 0.02 kcal/mol, and 0.414, respectively, (see Table IV). The values of ΔG_b and ΔS_b were also calculated and listed in Table IV. The binding stoichiometry, *n* = 0.414, suggests that every DS monomer binds to $1/n$ = 2.4 VRP molecules. This result is consistent with the nominal number of sulfate groups (2.3) available in each monomer unit of DS described by the supplier.

In addition, form Table IV, it can be found that both enthalpy and entropy favor the ionic complexation of VRP and DS as $\Delta H_b < 0$ and $\Delta S_b > 0$. Although ΔH_b is two-order magnitude of that of ΔS_b (0.014 kcal mol^{-1} K^{-1}) indicating that the complexation is an enthalpically driven process, the two terms of ΔH_b and $-T\Delta S_b$ are comparable (i.e., -4.9 *versus* -4.1).

Thermal Phase Transition and Crystallinity

Figure 5 compares the DSC thermograms of VRP (curve A), DA (curve B), DS (curve C), physical mixture of VRP and DS (curve D), VRP-DS complex (curve E) and DA containing VRP-DS complex (curve F). The ionic molar ratio of DS/VRP in the mixture and the complex was fixed at 1.0. The results show that both VRP and DA alone are in crystalline forms, while DS is in an amorphous form. VRP decomposed at 152.80°C, ~7°C above its melting temperature, and DS decomposed at 132.50°C. In the physical mixture of VRP and DS, the melting point of VRP is shifted significantly from 145.47°C, its original melting point (curve

Table III. Drug Loading Efficiency and Loading Capacity at Different Weight Ratios of Drug to Dodecanoic Acid (DA) as Lipid Carrier in the Apparent Partition Coefficient Experiment

Nominal VRP/DA ratio (w/w)	Drug loading efficiency (%)*	Drug loading capacity (%)**
1:25	98.91 ± 0.43	3.95 ± 0.017
1:10	96.84 ± 0.60	9.63 ± 0.084
1:5	96.92 ± 1.48	19.31 ± 0.26
1:3.3	95.52 ± 1.29	28.55 ± 0.39
1:2	97.14 ± 0.77	48.46 ± 0.42
1:1	88.48 ± 2.35	88.07 ± 2.24

The ionic molar ratio of DS to VRP was fixed at 1.0.
The values are the mean ± S.D. of triplicate.
* calculated using Eq. (9).
** calculated using Eq. (10).

A), to 114.05°C (curve D) due to its strong interactions with DS. Moreover, the endothermic peak of VRP becomes broader and blunt. While crystalline VRP still exists in the physical mixture, the VRP in the lyophilized VRP-DS complex sample is in an amorphous form as indicated by the absence of the melting peak of VRP in curve D. Similar to DS, decomposition of the complex occurred at 132°C (data not shown). A glass transition temperature of DS at 61.7°C in the lyophilized VRP-DS complex is seen in curve E, which is however not detected in the DS alone (curve C) and the physical mixture sample (curve D). In addition, a very small exothermic peak at 106.96°C is noticed in the thermogram of VRP-DS complex (curve E). In the complex loaded lipid formulation, the crystalline form of DA remains, yet the VRP becomes amorphous, evidenced by the absence of its endothermic peak (curve F). However, the melting peak of DA becomes broader and decreases from 45.24°C for the lipid alone to 43.38°C for the complex included formulation.
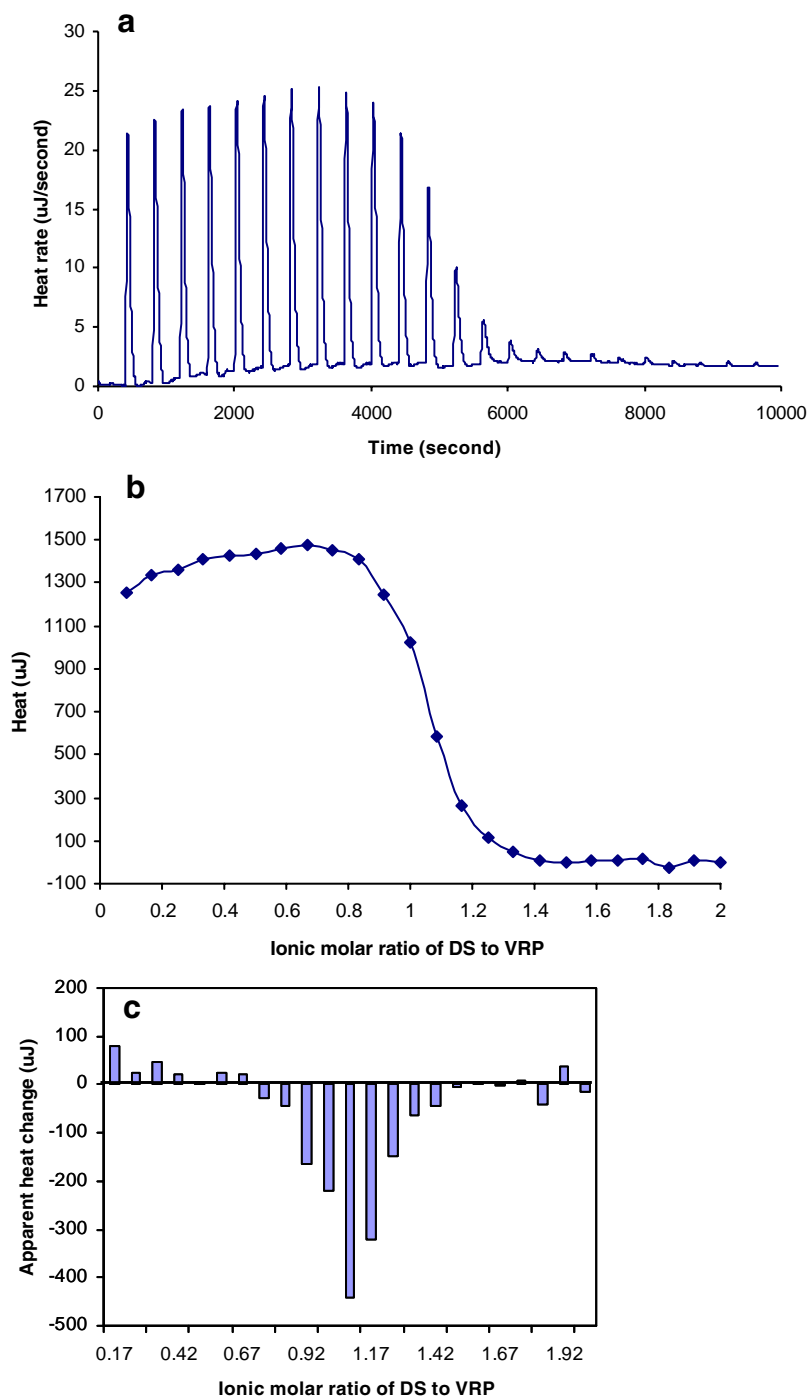

Fig. 3. (a) Primary ITC data for VRP-DS complexation; (b) Calibrated heat generated by titration of VRP with DS *versus* ionic molar ratio of DS toVRP and (c) apparent heat change against ionic molar ratio of DS to VRP.
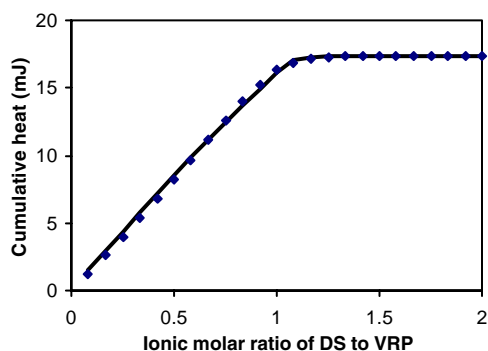
Fig. 4. Data fitting (*line*) of cumulative heat (*symbols*) *versus* the ionic molar ratio of DS to VRP by using the combination of Eqs. (7) and (8) (see text).

Table IV. Thermodynamic Parameters for DS Complexation with VRP at 25°C

Parameters	Value
K_b, 10^6 M^{-1}	3.6
ΔG_b, kcal mol^{-1}	−8.9
ΔH_b, kcal mol^{-1}	−4.9 ± 0.06
ΔS_b, cal mol^{-1} K^{-1}	13.7 ± 0.003
n	0.414

The enthalpies of the DA melting were calculated by using the area of the melting peak of DA divided by the total weight of the samples for DSC analysis. As illustrated in Table V, when compared with the melting enthalpy of pure DA (137.70 J/g), incorporation of 88% complex leads to the depression of melting enthalpy of DA to 60.34 J/g. Taking the enthalpy of pure DA as being 100%, the crystallinity of the complex incorporated DA is estimated to be 43.82% (31,32). However, this value is close to the lipid weight percent in the sample, i.e., 46.2%. Hence the reduction in the crystallinity is mainly caused by the decrease in the DA content.

The diffractograms of all samples shown in Fig. 6 further confirmed the results of DSC thermal analysis. VRP is in the crystalline state with strong diffractions at 4.65°, 14.44°, 18.82° and 23.60° (Fig. 6-1). Dodecanoic acid has sharp crystalline peaks at 3.00°, 6.40°, 9.66°, 21.51° and 23.88° (Fig. 6-2). The extremely strong first peak defines the interlayer distance of 27.4 Å suggesting a layered crystal structure. DS is an amorphous material without any diffrac-
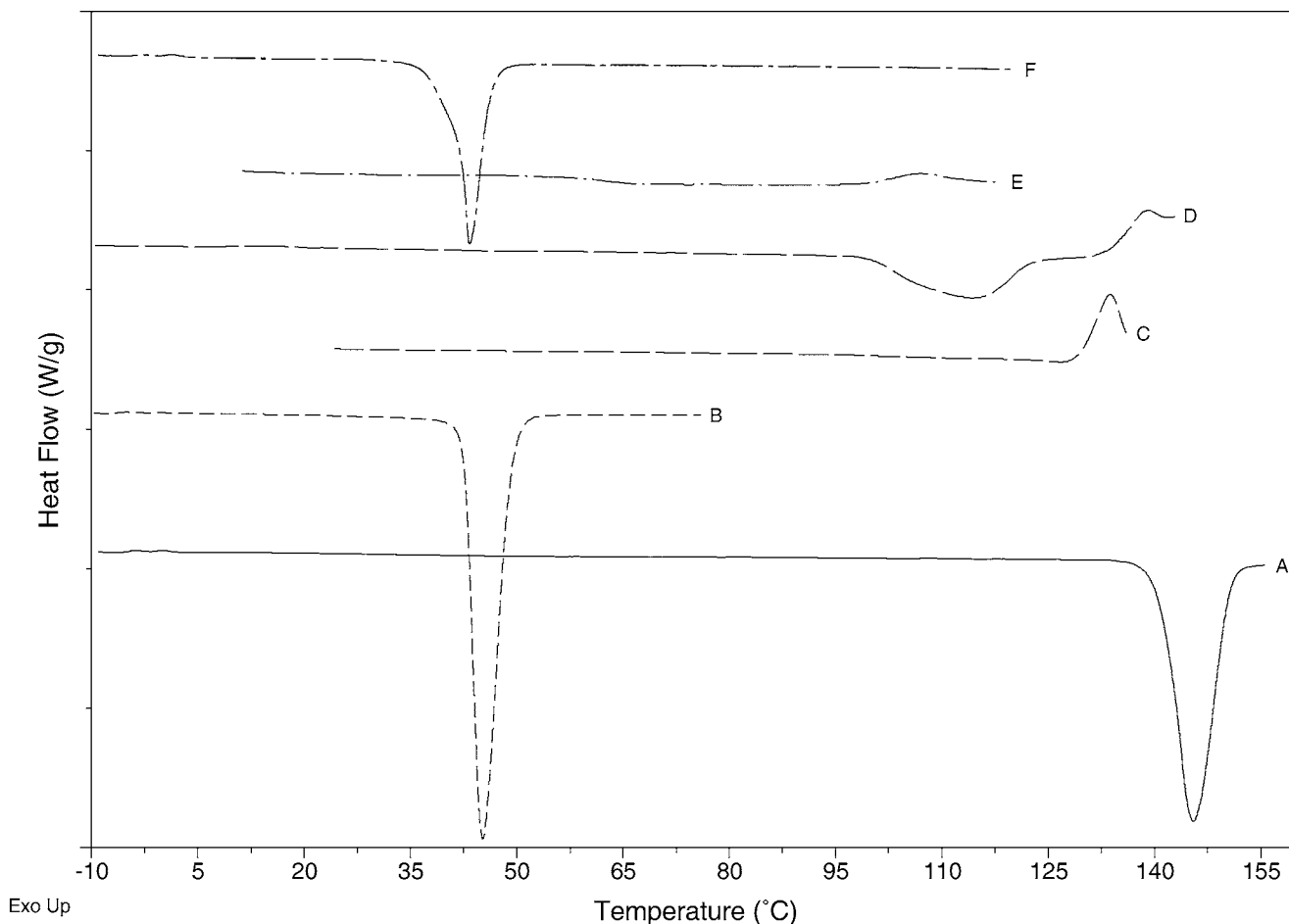

Fig. 5. Differential scanning calorimetry thermograms of (A) verapamil HCl; (B) dodecanoic acid; (C) dextran sulfate sodium salt; (D) physical mixture of verapamil HCl and dextran sulfate sodium salt; (E) VRP-DS complex and (F) dodecanoic acid containing VRP-DS complex. The ionic molar ratio of DS to VRP in samples of (D), (E) and (F) was fixed at 1.0.

Table V. Melting Points, Enthalpies and Crystallinity of Pure Lipid DA and the Lyophilized VRP-DS Complex Incorporated DA where Drug/Lipid Weight Ratio=1.0 and Ionic Molar Ratio of DS/VRP=1.0

Parameter	Pure DA	VRP-DS complex loaded DA
Melting peak (°C)	45.24	43.38
Enthalpy (J/g)	137.70	60.34
Crystallinity (%)	100.00	43.82

The melting enthalpies were calculated based on the total weight of the samples for DSC analysis (pure DA or VRP-DS complex loaded DA). The melting enthalpy of pure DA was used as reference (100% of crystallinity), from which the crystallinity of VRP-DS complex loaded lipid was calculated as the percentage of the enthalpy to that of pure DA. The weight percent of DA in the complex loaded formulation was 46.2%.

tion (Fig. 6-3). In comparison with the diffractogram of VRP alone, the higher overall background of the diffraction pattern of VRP-DS physical mixture demonstrated that it was a mixture of crystalline VRP and amorphous DS (Fig. 6-4). The absence of any shifts in characteristic peaks of VRP or the presence of new peaks suggested that no change occurred in the crystal structures of VRP or amorphous structure of DS in this mixture. Figure 6-5 shows that that overall the lyophilized complex is an amorphous material. The small peak at 4.17° (2θ) indicates the possibility of a small amount of crystals exists in the complex. However, no characteristic peaks of VRP were detected in the complex sample (Fig. 6-5), suggesting that VRP is essentially in an amorphous form in the VRP-DS complex.

Considering the appearance of a small exothermic peak in the thermogram of VRP-DS complex (Fig. 5 curve E), it is possible that a tiny amount of unbound VRP resided inside the VRP-DS gel after washing, which may form complex with DS thus releasing heat when the polymer chains become more flexible at temperatures above the glass transition temperature. However, the residual VRP would have been randomly distributed among the chains of VRP-DS complex since no characteristic peaks appeared in the X-ray diffractogram. The pattern of VRP-DS complex incorporated dodecanoic acid confirmed that it was a mixture of DA in a crystalline form and the VRP-DS complex in an amorphous form suggested by the significantly higher background of the PXRD graph (Fig. 6-6) as compared to that for DA alone.
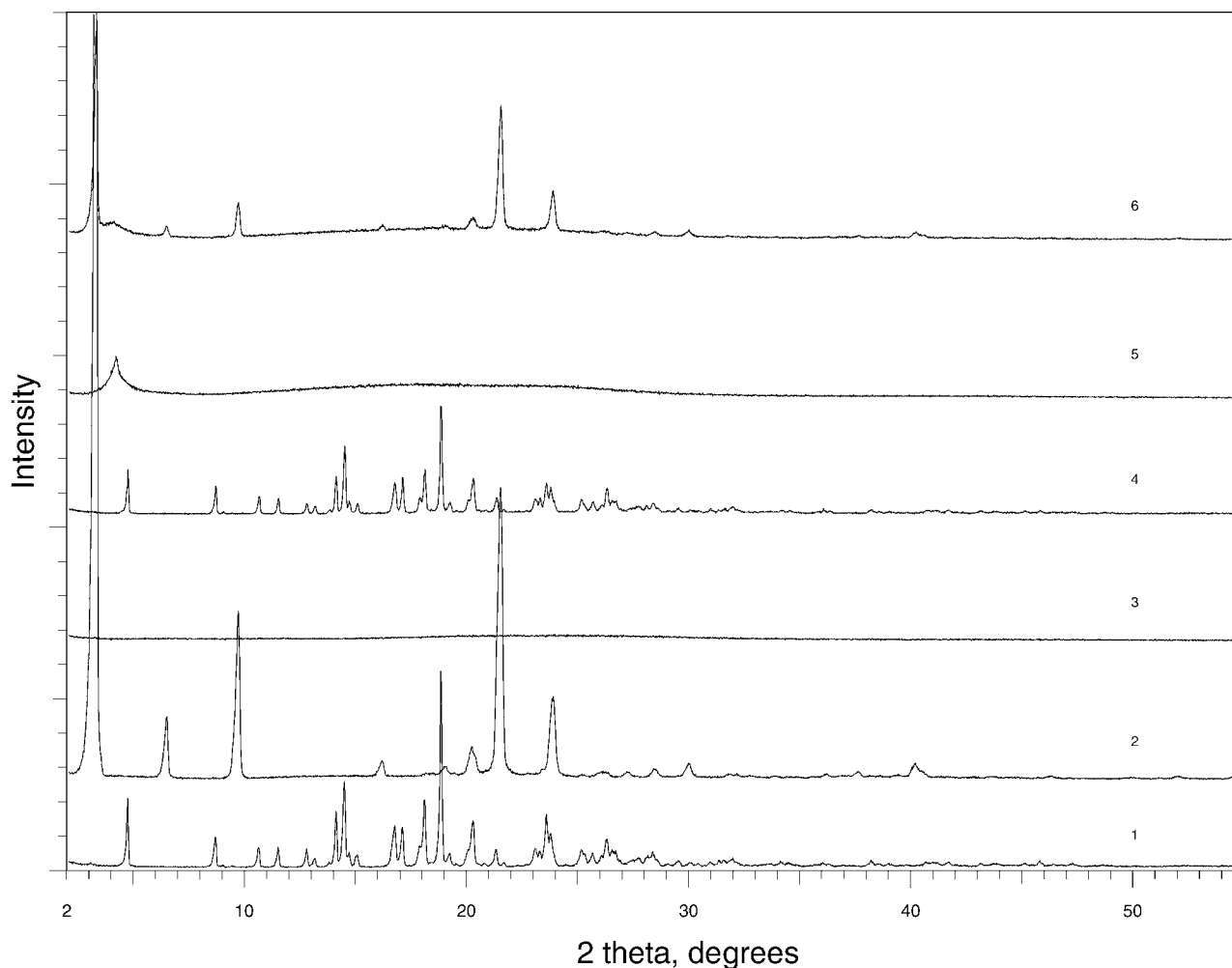

Fig. 6. Overlaid powder X-ray diffraction crystallographs of **1** verapamil HCl; **2** dodecanoic acid; **3** dextran sulfate sodium salt; **4** physical mixture of verapamil HCl and dextran sulfate sodium salt; **5** VRP-DS complex; **6** VRP-DS complex incorporated dodecanoic acid.

DISCUSSION

Best Lipid Candidate

Based on the calculated total solubility parameter, enthalpy of mixing and polarity of various lipids and the VRP-DS complex (Tables I and II), DA was identified as the lipid which would achieve maximum miscibility with the complex. This finding was verified by partition experiments where the complex showed the strongest partition in DA. The mutual miscibility between DA and the complex stems from the existence of many polar groups in the complex. Considering the enthalpy of mixing, a trend was highlighted that the increasing differences of total solubility parameter and polarity correspond to the increasing incompatibility/immiscibility between the complex and lipid carriers.

Influence of DS/VRP Ionic Molar Ratio

The partition study revealed that the partition of VRP and VRP-DS complex in lipid phase largely depended on the ionic molar ratio of DS to VRP. The highest partition coefficient of VRP was obtained at unity DS/VRP ionic molar ratio (Fig. 2), at which the highest hydrophobicity and binding efficiency of DS was likely to be achieved. At DS/VRP < 1.0, the neutralization of present VRP charges was incomplete leaving unbound, ionic VRP molecules in the aqueous phase. At DS/VRP = 1.0, the neutralization of charges in both DS and VRP was virtually complete. Hence the complex exhibited the highest affinity to the lipid. At DS/VRP > 1.0, DS molecules competed for binding with VRP, leading to incomplete neutralization of sulfate groups in DS molecules. Thus the complex, carrying residual negative charges, had higher hydrophilicity thereby lower lipid partition. This interpretation was supported by the results from ITC. As shown in Fig. 4, cumulative heat released increased linearly with the DS/VRP ionic molar ratio from 0.08 to 1.0 (r^2 = 0.998), demonstrating that nearly all the DS was complexed with VRP. The subsequent plateau suggested that VRP in the solution was depleted and thus no more heat was generated.

The complete neutralization of DS indicates that the binding sites distributed in DS molecules can be bound freely with the drug molecule, probably due to the relatively short chain length and a low degree of branching (< 5%) of DS. Steric restriction seems to have negligible effect on the VRP-DS binding. Therefore, VRP-DS association can be considered as an independent process. At each binding site, a simple equilibrium exists between drug (VRP$^+$), polymer (DS–SO$_3^-$) and drug-polymer complex (DS–SO$_3^-$VRP$^+$):

$$DS - SO_3^- + VRP^+ \rightleftharpoons DS - SO_3^- VRP^+ \qquad (11)$$

At DS/VRP=1.0, the maximum binding capacity of DS is 6.28 μmol/mg, corresponding to 75.5% (w/w) drug loading in the complex.

Influence of PLN Components on the Solid State Properties

DSC and PXRD results indicated that VRP was amorphous in the lyophilized VRP-DS complex, which may be ascribed to the isolation effect of amorphous DS molecules. The tight binding of VRP molecules with the sulfate groups in the disordered DS molecules prevents VRP from forming crystalline structure. The complex and DS decomposition a temperatures ~132°C suggested that the complexation of DS with VRP did not destabilize nor stabilize the polymer.

Depression of the melting point of the complex incorporated DA from 45.24 to 43.38°C revealed distortion of the crystalline structure of DA in the presence of the complex. Nevertheless, both components were still compatible with each other since the characteristic peaks of DA remained in the PXRD pattern (Fig. 6-6). Since only the complex was incorporated in the lipid matrix, it is conceivable that the complex disturbs the crystal formation of DA because of their mutual solubility/miscibility. In addition, the amorphous state of VRP-DS complex would also favor its solubility in lipids.

The very small exothermic peak at 106.96°C in the thermogram of VRP-DS complex has an enthalpy of −0.071 J (Fig. 5 curve E). The exothermic nature of this peak precludes the evaporation of residual water. Moreover, decomposition of free polymer or the complex could not explain the appearance of such a small peak. Considering the enthalpy of DS binding with VRP, ΔH_b=−4.9 kcal/mol, the small exothermic peak might be due to the binding of a small amount of residual VRP randomly dispersed in the complex to the sulfate groups of free DS molecules also entrapped in the complex. Mobility of the complex increases with heating, which enables the intimate contact between the residual drug and polymer. This explanation was further supported by the absence of such a peak in the second and third cycle of thermal scanning of the same sample (data not shown) as the residual free VRP molecules had already bounded to the DS in the first cycle.

CONCLUSION

DA was identified as a promising lipid candidate for PLN based on the analyses of solubility parameters and partition coefficients. The mutual solubility between the complex and DA resulted in a slight decrease in the melting point of DA while the crystalline structure remained. After complexation with DS, VRP became amorphous, which, together with the good miscibility of the complex and DA, led to high drug loading capacity of the lipid. DS to VRP binding is a thermodynamically favorable, enthalpy-driven process. At the equal ionic molar ratio of DS to VRP, both the maximum binding efficiency of DS and the highest drug loading capacity of DA were obtained.

Based on the findings in this work, a PLN system using DA as a lipid carrier has been formulated. Further physicochemical characterization and a study of *in vitro* release kinetics and release mechanism of the formulation are now in progress. Although the present work manifests the suitability of solubility parameters theory in the screening of lipid carriers of PLN, its usefulness for regular SLN incorporating hydrophobic drugs will require further exploration.

ACKNOWLEDGMENTS

REFERENCES

1. R. H. Müller, S. Maaßen, H. Weyhers, F. Specht, and J. S. Lucks. Cytotoxicity of magnetite loaded polylactide, polylactide/glycolide particles and solid lipid nanoparticles (SLN). *Int. J. Pharm.* **138**:85–94 (1996).

2. C. Schwarz, W. Mehnert, J. S. Lucks, and R. H. Müller. Solid lipid nanoparticles (SLN) for controlled drug delivery. I. Production, characterization and sterilization. *J. Control. Release* **30**:83–96 (1994).

3. R. H. Müller, W. Mehnert, J. S. Lucks, C. Schwarz, A. zur Muhlen, H. Weyhers, C. Freitas, and D. Ruhl. Solid lipid nanoparticles (SLN)–an alternative colloidal carrier system for controlled drug delivery. *Eur. Pharm. Biopharm.* **41**:62–69 (1995).

4. S. A. Wissing, O. Kayser, and R. H. Müller. Solid lipid nanoparticles for parenteral drug delivery. *Adv. Drug Deliv. Rev.* **56**:1257–1272 (2004).

5. W. Mehnert and K. Mader. Solid lipid nanoparticles, production, characterization and applications. *Adv. Drug Deliv. Rev.* **47**:165–196 (2001).

6. K. Westesen, H. Bunjes, and M. H. J. Koch. Physicochemical characterization of lipid nanoparticles and evaluation of their drug loading capacity and sustained release potential. *J. Control. Release* **48**:223–236 (1997).

7. V. Jenning and S. Gohla. Comparison of wax and glyceride solid lipid nanoparticles (SLN). *Int. J. Pharm.* **196**:219–222 (2000).

8. R. Cavalli, S. Morel, M. R. Gasco, P. Chetoni, and M. F. Saettone. Preparation and evaluation *in vitro* of colloidal lipospheres containing pilocarpine as ion pair. *Int. J. Pharm.* **117**:243–246 (1995).

9. G. P. Zara, R. Cavalli, A. Fundaro, A. Bargoni, O. Caputo, and M. R. Gasco. Pharmacokinetics of doxorubicin incorporated in solid lipid nanoparticles (SLN). *Pharm. Res.* **40**:281–286 (1999).

10. R. Cavalli, M. R. Gasco, P. Chetoni, S. Burgalassi, and F. M. Saettone. Solid lipid nanoparticles (SLN) as ocular delivery system for tobramycin. *Int. J. Pharm.* **238**:241–245 (2002).

11. H. L. Wong, R. Bendayan, A. M. Rauth, and X. Y. Wu. Development of solid lipid nanoparticles containing ionically complexed chemometherapeutic drugs and chemosensitizers. *J. Pharm. Sci.* **93**:1993–2008 (2004).

12. H. L. Wong, A. M. Rauth, R. Bendayan, and X. Y. Wu. A new solid lipid nanoparticle formulation increases cytotoxicity of doxorubicin against multidrug-resistant human breast cancer cells. *Pharm. Res.* In press.

13. H. L. Wong. Ph.D. dissertation, University of Toronto, Canada, 2006.

14. R. C. Rowe. Polar/nonpolar interactions in the granulation of organic substrates with polymer binding agents. *Int. J. Pharm.* **56**:117–224 (1989).

15. D. J. Greenhalgh, A. C. Williams, P. Timmins, and P. York. Solubility parameters as predictors of miscibility in solid dispersions. *J. Pharm. Sci.* **88**:1182–1190 (1999).

16. S. Schenderlein, M. Lück, and B. W. Müller. Partial solubility parameters of poly(D,L-lactide-co-glycolide). *Int. J. Pharm.* **286**:19–26 (2004).

17. R. H. Müller, K. Mader, and S. Gohla. Solid lipid nanoparticles (SLN) for controlled drug delivery—a review of the state of art. *Eur. J. Pharm. Biopharm.* **50**:161–177 (2000).

18. P. Bummer. Physical chemical considerations of lipid-based oral drug delivery-solid lipid nanoparticles. *Crit. Rev. Therap. Drug Carr. Syst.* **21**:1–19 (2004).

19. P. Mura, A. Manderrioli, G. Bramanti, S. Furlanetto, and S. Pinzauti. Utilization of differential scanning calorimetry as a screening technique to determine the compatibility of ketoprofen with excipients. *Int. J. Pharm.* **119**:71–79 (1995).

20. G. A. G. Novoa, J. Heinämäki, S. Mirza, O. Antikainen, A. I. Colarte, A. S. Paz, and J. Yliruusi. Physical solid-state properties and dissolution of sustained-release matrices of polyvinylacetate. *Eur. J. Pharm. Biopharm.* **59**:343–350 (2005).

21. B. Hancock, P. York, and R. C. Rowe. The use of solubility parameters in pharmaceutical dosage form design. *Int. J. Pharm.* **148**:1–21 (1997).

22. J. Barra, P. Bustamante, and E. Doelker. Use of the solubility parameter and surface energy concepts in the formulation of solid dosage forms. *S.T.P. Pharm. Sci.* **9**:293–305 (1999).

23. J. L. Garson. The influence of polarity on the solubility parameter concept. *J. Paint Technol.* **38**:43–57 (1966).

24. R. F. Fedors. A method for estimating both the solubility parameters and molar volumes of liquids. *Polymer Engin. Sci.* **14**:147–154 (1974).

25. D. W. Van Krevelen. Cohesive properties and solubility. In D. V. Van Krevelen D. V. Van Krevelen (ed)., *Properties of Polymers: Their Correlation with Chemical Structure; Their Numerical Estimation and Prediction from Additive Group Contribution*. Elsevier, New York, 1990, pp. 189–224.

26. I. Jelesarov and H. R. Bosshard. Isothermal titration calorimetry and differential scanning calorimetry as complementary tools to investigate the energetics of biomolecular recognition. *J. Mol. Recognit.* **12**:3–18 (1999).

27. C. M. Hansen. The three dimensional solubility parameters—key to paint component affinities. 1. Solvents, plasticizers, polymers and resins. *J. Paint Technol.* **39**:104–117 (1967).

28. R. C. Rowe. Interactions of lubricants with microcrystalline cellulose and anhydrous lactose—a solubility parameter approach. *Int. J. Pharm.* **41**:223–226 (1988).

29. G. Puglisi, N. A. Santagati, R. Pignatello, C. Ventura, F. A. Bottino, S. Mangiafico, and G. Mazzone. Inclusion complexation of 4-biphenylacetic acid with β-cyclodextrin. *Drug Dev. Ind. Pharm.* **16**:395–413 (1990).

30. F. Han, N. Taulier, and T. V. Chalikian. Association of the minor groove binding drug Hoechst 33258 with d(CGCGAATTCGCG)$_2$: volumetric, calorimetric, and spectroscopic characterizations. *Biochem.* **44**:9785–9794 (2005).

31. A. zur Mühlen, C. Schwarz, and W. Mehnert. Solid lipid nanoparticles (SLN) for controlled drug delivery—drug release and release mechanism. *Eur. J. Pharm. Biopharm.* **45**:149–155 (1998).

32. C. Freitas and R. H. Müller. Correlation between long-term stability of solid lipid nanoparticles (SLN™) and crystallinity of the lipid phase. *Eur. J. Pharm. Biopharm.* **47**:125–132 (1999).